Table 2. In three separate experiments C6-2B cells were incubated with the protein or RNA synthesis inhibitors for 24 hours. The intracellular cyclic AMP accumulation in response to a 30-minute challenge with 100 μM forskolin or 10 μM (−)-isoproterenol is indicated. Results are means ± S.E.M. for three determinations.

Treatment	Cyclic AMP (pmole/mg)		
	Control	Forskolin	Isoproterenol
None	55 ± 6	4075 ± 277	5866 ± 110
Cycloheximide (5 μg/ml)	52 ± 4	831 ± 127	3951 ± 118
None	61 ± 9	4473 ± 177	5224 ± 210
Emetine (1 μg/ml)	55 ± 3	848 ± 71	3860 ± 238
None	24 ± 2	2686 ± 114	5572 ± 295
DRB (100 μM)	23 ± 8	3004 ± 30	5124 ± 374

proterenol was unaltered after 8 hours of cycloheximide treatment and was decreased about 35 percent after 24 hours. The responsiveness of the cells to cholera toxin was unaltered after 24 hours of cycloheximide treatment (Table 1).

Incubation of cells for 24 hours with emetine, another protein synthesis inhibitor, gave results similar to those obtained with cycloheximide (Table 2). However, treatment of the cells for up to 24 hours with the RNA synthesis inhibitor 5,6-dichloro-1-β-D-ribofuranosylbenzimidazole (DRB) caused no loss of cellular responsiveness to (−)-isoproterenol, cholera toxin, or forskolin (Table 2). Incubation of the cells with cycloheximide or emetine caused a 93 percent and 95 percent inhibition of [^{3}H]leucine incorporation, respectively, and had no effect on [^{3}H]uridine incorporation. An 85 percent inhibition of RNA synthesis, but no inhibition of protein synthesis, was observed with DRB treatment.

The more labile component of the cyclase system required for forskolin-stimulated cyclic AMP accumulation identified by these experiments is unlikely to be the β-adrenergic receptor, the guanine nucleotide regulatory component, or the catalytic component of cyclase. Cyclic AMP production stimulated by cholera toxin or the β receptor was either unaltered or slightly reduced after an 8- to 24-hour incubation with cycloheximide, yet these conditions reduced the responsiveness of the cells to forskolin by 65 to 85 percent. If it is assumed that forskolin directly stimulates the catalytic subunit of cyclase, it is difficult to reconcile a linear model of the hormone-sensitive adenylate cyclase with these data.

There are, however, several other ways to interpret these data. The cyclase catalytic unit involved in forskolin-stimulated cyclase activity may differ from the one necessary for hormone- or cholera toxin–stimulated cyclic AMP accumulation. Another possibility is that forskolin stimulates adenylate cyclase activity through a regulatory protein not necessary for hormone- or cholera toxin–stimulated cyclase activity. Our experiments do not differentiate between these two possibilities. However, we can conclude that the message for the putative protein is long-lived because inhibition of RNA synthesis for 24 hours did not reduce the responsiveness of forskolin, and the half-life of the protein is probably shorter than those of the β-adrenergic receptor, G/F, or catalytic cyclase.

GARY BROOKER
CAROLYN PEDONE
KENNETH BAROVSKY
Department of Biochemistry, Georgetown University Medical Center, Washington, D.C. 20007

References and Notes

1. E. M. Ross and A. G. Gilman, *Annu. Rev. Biochem.* **49**, 533 (1980).
2. J. K. Northup *et al.*, *Proc. Natl. Acad. Sci. U.S.A.* **77**, 6516 (1980).
3. K. B. Seamon and J. W. Daly, *J. Cyclic Nucleotide Res.* **7**, 201 (1981).
4. G. L. Johnson, H. R. Kaslow, H. R. Bourne, *J. Biol. Chem.* **253**, 7120 (1978).
5. K. B. Seamon, W. Padgett, J. W. Daly, *Proc. Natl. Acad. Sci. U.S.A.* **78**, 3363 (1981).
6. W. L. Terasaki and G. Brooker, *J. Biol. Chem.* **253**, 5418 (1978).
7. J. F. Harper and G. Brooker, *J. Cyclic Nucleotide Res.* **1**, 207 (1975).
8. G. Brooker, W. L. Terasaki, M. G. Price, *Science* **194**, 270 (1976).
9. G. A. Nickols and G. Brooker, *J. Biol. Chem.* **255**, 23 (1980).
10. Supported by NIH grants HL 28940 and HL 06330.

18 October 1982; revised 30 November 1982

In vivo One-Dimensional Imaging of Phosphorus Metabolites by Phosphorus-31 Nuclear Magnetic Resonance

Abstract. *A phosphorus-31 nuclear magnetic resonance imaging technique has been used to obtain information on phosphorus metabolites from different spatial regions of tissues in vivo. The technique for selection of planes through the tissue is based on phase-encoding of spin echoes and was used to obtain one-dimensional discrimination of phosphorus-31 spectra from different parts of the tissue simultaneously. Specimens were resolved into 16 distinct slices and a signal-to-noise ratio of about 20 to 1 was obtained in ½ hour. Results are presented for phantoms, rat legs, and gerbil heads.*

Phosphorus-31 muclear magnetic resonance (^{31}P NMR) is a valuable noninvasive method for investigating the metabolic state of tissues in vivo (*1–3*). In order to realize the full potential of the method, it will be important to be able to discriminate different spatial regions of the tissue. Topical magnetic resonance (*4*) with surface coils has been used for this purpose (*5*), but a more versatile approach would be to use NMR imaging techniques to discriminate spatially different regions of the tissue simultaneously. Although there have been speculations, based on images of phantoms, about the possibility of using ^{31}P NMR imaging in vivo (*6, 7*), to our knowledge this is the first report of experimental in vivo ^{31}P NMR imaging.

There are two main differences between ^{31}P NMR imaging and the rather well-developed techniques of proton imaging which prevent the direct use for ^{31}P measurement of the techniques developed for ^{1}H. First, the concentration of ^{31}P metabolites in tissues is about 10^4 to 10^5 times lower than the proton concentration. Second, the biochemical information in ^{31}P signals can be obtained only under "high-resolution" conditions; that is, one must be able to distinguish the ^{31}P NMR signals from different metabolites, say by chemical shift differences. Spatial and spectral resolution of the "high-energy" phosphate metabolites, such as adenosine triphosphate (ATP) and phosphocreatine (PCr), and the "low-energy" phosphate metabolites, such as inorganic phosphate (Pi) and sugar phosphates (SP), will yield valuable information about the state of the tissue. Hence it is of practical importance to study the whole spectrum at each part of the tissue. We describe here a technique for simultaneously recording the ^{31}P NMR spectra from different planes through the tissue and present our results for rat legs and gerbil heads.

Nuclear magnetic resonance spectra at 1.4 T were recorded with a John-

son Foundation NMR spectrometer equipped with an Oxford Instruments 7-inch bore magnet (*8*). The spectral frequency for ^{31}P was 24.3 MHz. A single Helmholtz radio-frequency (RF) coil (a two-turn split coil RF probe with a coil separation of 25 mm) was used for excitation and detection. One-dimensional imaging was performed by a phase-encoded spin echo method, as illustrated in Fig. 1. A spin echo is formed by applying a 90° pulse followed by a 180° pulse. During the time period T between the two pulses, a pulsed magnetic field gradient (for instance, G_x) is applied to the specimen. This gradient causes the ^{31}P spins at each point along the gradient direction (in this case the x axis) to precess with different Larmor frequencies so that, at the time of application of the 180° pulse, the phase of each spin component will depend on its position. The spins are thus phase-encoded with respect to their positions. The echoes are collected at zero gradient so that precession frequency again depends only on the chemical shift. A series of N different echoes are collected, corresponding to N equally incremented phase-encoding G_x values. The complete sequence of N echoes is repeated a number of times for signal averaging. Because we make use of the phase information, the spatial transform is analogous to conventional NMR data with quadrature detection in that N independent echos are needed for N spatial slices.

The echoes $s(G,t)$ are subjected to a two-dimensional Fourier transformation to yield spectra as a function of position along the x axis, $S(x,v)$, and the absolute value of S is plotted to avoid problems due to different phase relations between different regions of our objects. The spatial resolution and total field of view are related to the number and values of the field gradients by the characteristics of the digital, discrete Fourier transforms in a manner similar to that in which the spectral resolution and sweep width are related to the temporal sampling of the free induction decay or echo. Thus, consider a case in which N echoes are obtained at N different field gradients with values equally spaced by ΔG_x (hertz per centimeter); the total unique field of view in space is given by

$$X_{\text{total}} = \frac{1}{\Delta G_x T} \text{ (cm)}$$

where T is the time period for which the field gradient is applied. One could equally well increment T with a constant gradient value. Any NMR signals originating from outside the total field of view will be "aliased" to appear to originate

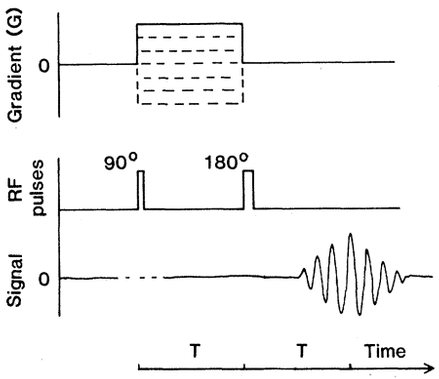

Fig. 1. Schematic diagram of the pulse and gradient sequence used for phase-encoded phosphorus imaging.

from within it. It is thus useful to set the gradient increment ΔG_x small enough that X_{total} is just slightly larger than the total sample. Typically, for these spectra, successive gradients differed by ΔG_x on the order of 10 Hz/cm per step. The spatial resolution will be given by

$$X_{\text{slice}} = \frac{X_{\text{total}}}{N}$$

and represents the size of the smallest spatial element from which we can obtain a unique spectrum. When calculating the Fourier transform, the N echoes may be "zero filled" to N' echoes; this procedure does not alter the total field of view or the intrinsic resolution but will yield N' spectra rather than N. The increased number of spectra arises from interpolation of the spectra for N unique spatial elements. In practice, the N different echoes are collected with both negative and positive gradients, one of the middle ones of the series being a null gradient.

Figure 2 shows the results of this imaging technique on a phantom. The phantom consisted of two test tubes (inner diameter, 7 mm) placed 15 mm apart, one containing 1 ml of 100 m*M* ATP (*p*H 7.0) and the other 1 ml of 100 m*M* phosphoric acid. Spin echoes were collected with T = 50 msec. Figure 2 shows a schematic outline of the phantom and of the spectra corresponding to the 16 slices throughout the phantom. The spatial resolution for the image is 3.3 mm, and the individual spectra from each tube are well resolved.

Figure 3 shows the results obtained

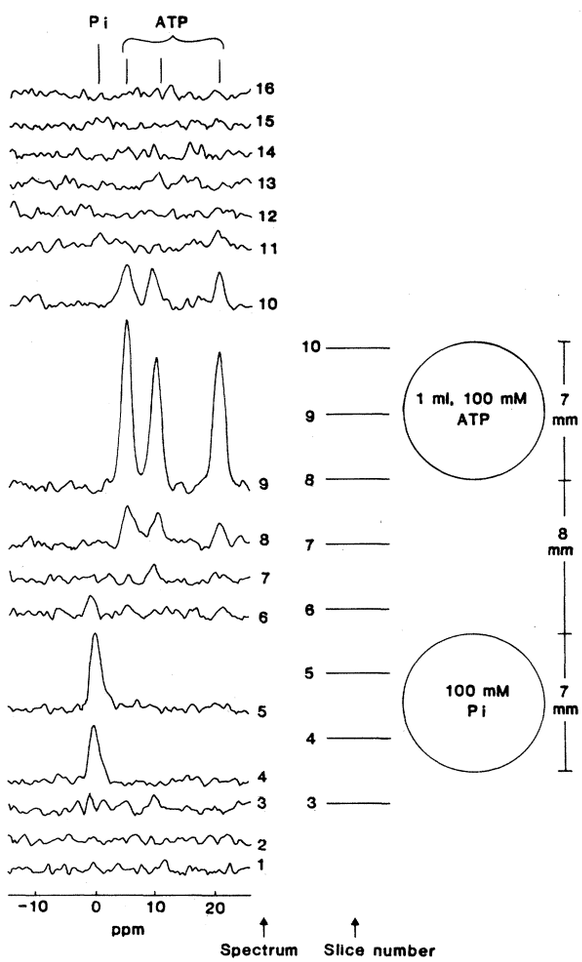

Fig. 2. Spectra recorded from a phantom consisting of two test tubes. Successive pulse sequences were separated by 4 seconds. Each echo was the sum of 25 repetitions and the total recording time was 26 minutes. The two-dimensional array (16 echoes with 608 points each) was subjected to two-dimensional Fourier transformation to yield 16 spectra with 512 points each. Each spectrum corresponds to a slice 3.3 mm thick: only part of each spectrum is displayed here. The plan of the phantom and the position of each spatial slice are shown at the right.

when the same technique was applied to a living animal model for which the results could be anticipated. A tourniquet was applied to one hind limb of a rat, and both hind limbs—the normal and the ischemic limb—were placed together in the NMR probe. One-dimensional imaging was performed along the direction between the two legs. Sixteen different echoes were collected; each echo was recorded 25 times during the total experimental time of 26 minutes. The gradient was applied for $T = 25$ msec. The effective spatial resolution was 3.3 mm. The spectra in Fig. 3 clearly reveal the difference between the two legs. The control leg has a strong PCr peak with no significant Pi, while the ischemic leg has very little PCr but has a broad Pi peak, possibly reflecting the presence of several compartments within each of the slices, each with a different *p*H and hence a different chemical shift (*9*). The signal-to-noise ratio for the data as measured by the ratio of the height of the PCr peak to the maximum background excursion from zero is about 20:1. We do not see any ATP peaks in our spectra from animals in vivo because the T_2 relaxation time of ATP in many tissues is sufficiently short (~ 10 msec) that the signal has virtually completely relaxed in the 50 msec between the initial 90° pulse and the formation of the echo. (ATP is present in the spectra recorded from the phantom in Fig. 2.)

The third example presented here is a gerbil head (Fig. 4). To discriminate between the right and left hemispheres of the gerbil brain, one carotid artery was occluded and the gerbil head was placed in the NMR probe. Because the NMR signals were weaker in this case than for the rat legs, only nine gradient values were collected (with an average of 100 scans on each echo) to give a spatial resolution of 5.8 mm; the time period T was 25 msec, the total acquisition time was 1 hour. One can very clearly discern the differences between the right and left halves of the gerbil head in Fig. 4.

In this model of stroke, both brain hemispheres are rendered slightly hypoxic by a diminution of the inspired oxygen from 20 to 10 percent and one hemisphere is made ischemic by unilateral occlusion of the common carotid artery. Because of the partially functional circle of Willis (*10*) in this gerbil, the oxygen delivery to the two hemispheres differs only slightly yet does give distinct differences in the ratio of the amplitudes (and areas) of the peaks of PCr and Pi in two hemispheres.

A few comments on the effect of T_2's on the NMR spectra obtained by our method are in order. As pointed out earlier, ATP signals are not observed in our in vivo spectra due to short T_2 (~ 10 msec). For the same reason, one does not see the ^{31}P signals from the less mobile skull bone of the gerbil head in Fig. 4. Since the T_2 values of intracellular PCr and Pi in tissues are nearly the same [~ 80 msec (*11*)], we do not perceive any problems in obtaining quantitative PCr/Pi ratios from our spectra. Hence, with better magnet homogeneity, one can readily obtain a map of PCr/Pi ratios in a living tissue with this technique.

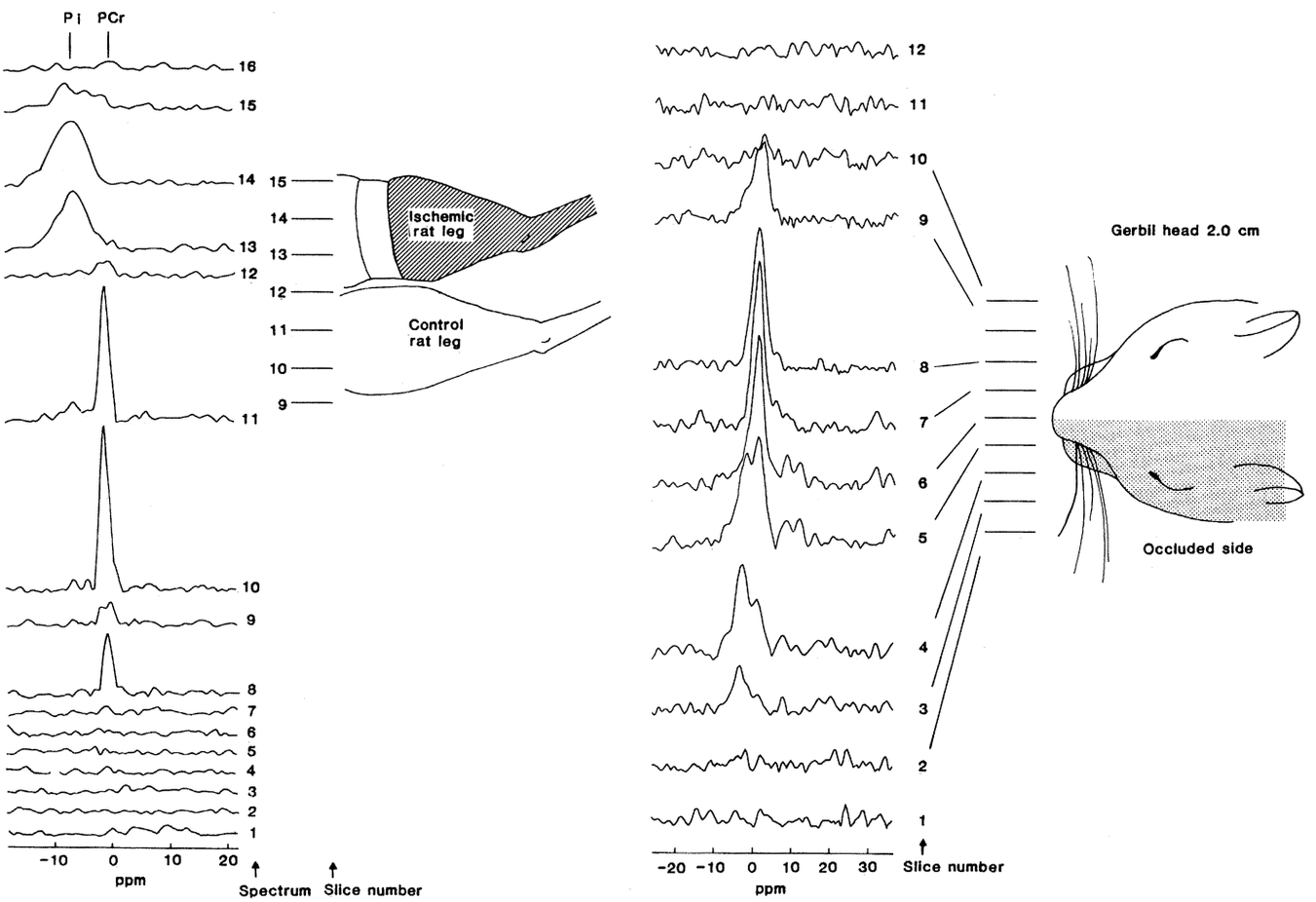

Fig. 3 (left). Spectra recorded from two rat legs. The delay between successive spectra was 4 seconds. The positions of the Pi and PCr peaks are indicated. Fig. 4 (right). Spectra recorded from a gerbil head in which the right carotid artery was occluded to form a unilateral ischemia. The gerbil head was placed in the homogeneous field of the magnet and the field gradient was applied along the axis connecting the ears of the gerbil. The data set was "zero-filled" to 16 echoes before transforming. The broad ^{31}P peak from the gerbil skull bone and the ATP peaks are not observed in this spectrum.

These results demonstrate the practicality of performing in vivo ^{31}P NMR spectral imaging. By using an imaging technique in which spatial information is encoded as the phase of an echo, it is possible to retain the spectral information needed for interpreting the phosphate metabolic information. The data presented here show that discrete spectra can be obtained in vivo from slices of tissue a few millimeters thick. No attempt was made to resolve different areas of each plane, but useful spectral signals must have originated from the animal tissue within the homogeneous region of the magnet, which in our case approximates a sphere of diameter 25 mm. Thus, for our resolution elements, the effective tissue volume of each slice is approximately 1 ml, for which we obtained a signal-to-noise ratio of about 20:1 in less than 1 hour.

We can use these results to predict the performance of metabolite imaging systems for larger (human) objects. We assume that we are able to scale up the linear dimensions of our present system fivefold in order to image human limbs. If the noise in our spectra arises predominantly from the RF coil, then the signal-to-noise ratio of a spectrum recorded from a volume V of tissue will be proportional to V/R, where R is the radius of the RF coil. Then if we wish to resolve a human limb to the same fractional resolution obtained for the rat, we may expect a volume element of approximately 125 ml. So for a 1-minute scan with a single 15-echo sequence, we may expect a signal-to-noise ratio of 100. Thus extension to two-dimensional slice information from human limbs and heads in times well under 1 hour seems readily possible.

There is no reason why this technique of spatially resolving metabolite spectra cannot be extended to three dimensions in vivo and to other nuclei such as ^{13}C and ^{23}Na.

J. C. HASELGROVE
V. HARIHARA SUBRAMANIAN
J. S. LEIGH, JR.
L. GYULAI
B. CHANCE

Johnson Research Foundation, Department of Biochemistry and Biophysics, University of Pennsylvania, Philadelphia 19104

References and Notes

1. C. T. Burt, S. M. Choen, M. Barany, *Annu. Rev. Biophys. Bioeng.* **8**, 1 (1979).
2. G. K. Radda and P. J. Seeley, *Annu. Rev. Physiol.* **41**, 749 (1979).
3. C. D'Ambrosio, B. Chance, J. S. Leigh, Jr., S. Eleff, in *Noninvasive Probes of Tissue Metabolism*, J. S. Cohen, Ed. (Wiley, New York, 1982), pp. 209–223.
4. R. E. Gordon, P. E. Hanley, D. Shaw, *Prog. Nucl. Magn. Reson. Spectrosc.* **15**, 1 (1982).
5. J. J. H. Ackerman, T. H. Grove, G. G. Wong, D. G. Gadian, G. K. Radda, *Nature (London)* **283**, 167 (1980).
6. P. Bendel, C. M. Lai, P. C. Lauterbur, *J. Magn. Reson.* **38**, 343 (1980).
7. T. R. Brown, B. M. Kincaid, K. Ugurbil, *Proc. Natl. Acad. Sci. U.S.A.* **79**, 3523 (1982).
8. B. Chance, S. Eleff, J. S. Leigh, Jr., *ibid.* **77**, 7430 (1981).
9. R. Moon and J. Richards, *J. Biol. Chem.* **248**, 7276 (1973).
10. S. Levine and H. Payan, *Exp. Neurol.* **16**, 255 (1966).
11. J. K. M. Roberts and O. Jardetsky, *Biochim. Biophys. Acta* **639**, 53 (1981).
12. We acknowledge with thanks the many people who have contributed to this effort, especially C. Barlow, S. Eleff, J. P. Idstrom, and J. Sorge.

3 February 1983; revised 30 March 1983

Hemoglobin Aggregation in Single Red Blood Cells of Sickle Cell Anemia

Abstract. *A laser light scattering technique was used to observe the extent of hemoglobin aggregation in solitary red blood cells of sickle cell anemia. Hemoglobin aggregation was confirmed in deoxygenated cells. The light scattering technique can also be applied to cytoplasmic studies of any biological cell.*

Polymerization of hemoglobin into fibers is a key phenomenon in sickle cell anemia (*1*). The red blood cells undergo reversible sickling and unsickling according to whether the hemoglobin is polymerized (deoxygenated) or depolymerized (oxygenated). The polymerization of hemoglobin in sickle cell anemia has been widely investigated, but in most cases cell-free solutions have been used (*1*). It is highly desirable to study the aggregation, nucleation, and polymerization of hemoglobin in intact red blood cells.

To make such observations, we have developed a laser light scattering apparatus for photon correlation spectroscopy under an optical microscope. Using this apparatus, we measured the Brownian motion of hemoglobin molecules inside a single red blood cell. The rate of the Brownian motion is directly proportional to the rate of intensity fluctuations of laser light scattered from the randomly moving hemoglobin molecules. The photon correlation technique is very sensitive to the slowing down of Brownian motion associated with dimerization, trimerization, and further aggregation of the hemoglobin molecules.

The experimental apparatus is shown in Fig. 1 (*2*). The beam of a He-Ne laser is expanded to a parallel beam 6 mm in diameter and then sharply focused into a

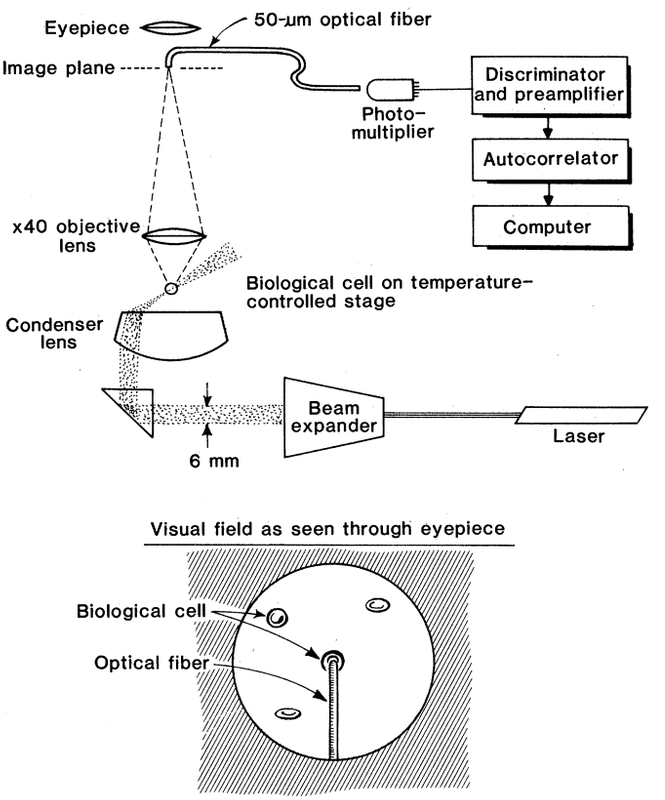

Fig. 1. Schematic diagram of the laser light scattering apparatus used to study the Brownian motion of a local region of cytoplasm in a single red blood cell. An optical fiber embedded in the eyepiece of the microscope collects only light scattered from a volume of 2 μm^3, allowing characterization of the extent of hemoglobin aggregation in the cell.